

# Ectopic expression of *Pax4* in pancreatic $\delta$ cells results in $\beta$ -like cell neogenesis

Noémie Druelle,<sup>1</sup> Andhira Vieira,<sup>1</sup> Aidin Shabro,<sup>1</sup> Monica Courtney,<sup>2</sup> Magali Mondin,<sup>1</sup> Samah Rekima,<sup>1</sup> Tiziana Napolitano,<sup>1</sup> Serena Silvano,<sup>1</sup> Sergi Navarro-Sanz,<sup>1</sup> Biljana Hadzic,<sup>1</sup> Fabio Avolio,<sup>1</sup> Mino Rassoulzadegan,<sup>1</sup> Herbert A. Schmid,<sup>3</sup> Ahmed Mansouri,<sup>4,5</sup> and Patrick Collombat<sup>1</sup>

<sup>1</sup>Université Côte d'Azur, Institut National de la Santé et de la Recherche Médicale, Centre National de la Recherche Scientifique, Institut Biologie Valrose, Nice, France

<sup>2</sup>EVOTEC International, Göttingen, Germany

<sup>3</sup>Novartis Pharmaceuticals, Basel, Switzerland

<sup>4</sup>Department of Molecular Cell Biology, Max Planck Institute for Biophysical Chemistry, Göttingen, Germany

<sup>5</sup>Department of Clinical Neurophysiology, University of Göttingen, Göttingen, Germany

The recent demonstration that pancreatic  $\alpha$  cells can be continuously regenerated and converted into  $\beta$ -like cells upon ectopic expression of *Pax4* opened new avenues of research in the endocrine cell differentiation and diabetes fields. To determine whether such plasticity was also shared by  $\delta$  cells, we generated and characterized transgenic animals that express *Pax4* specifically in somatostatin-expressing cells. We demonstrate that the ectopic expression of *Pax4* in  $\delta$  cells is sufficient to induce their conversion into functional  $\beta$ -like cells. Importantly, this conversion induces compensatory mechanisms involving the reactivation of endocrine developmental processes that result in dramatic  $\beta$ -like cell hyperplasia. Importantly, these  $\beta$ -like cells are functional and can partly reverse the consequences of chemically induced diabetes.

## Introduction

The endocrine pancreas is organized into highly vascularized functional units, termed islets of Langerhans, encompassing five endocrine cell subtypes ( $\alpha$ ,  $\beta$ ,  $\delta$ ,  $\epsilon$ , and pancreatic polypeptide cells) responsible for the secretion of glucagon, insulin, somatostatin, ghrelin, and pancreatic polypeptide, respectively (Adrian et al., 1978; Roncoroni et al., 1983; Prado et al., 2004). Type 1 diabetes mellitus is a metabolic disease resulting from the autoimmune-mediated loss of insulin-producing  $\beta$  cells. Such loss induces a chronic hyperglycemia, which, left untreated, could have grave vascular consequences (Morrish et al., 2001; Alwan, 2010; Pascolini and Mariotti, 2012). Despite current therapies (mostly exogenous insulin supplementation), patients with type 1 diabetes mellitus exhibit an overall shortened life expectancy and an altered quality of life because of their inability to strictly regulate glucose homeostasis (World Health Organization, 2016). Therefore, in a search for alternative treatments, approaches aiming at inducing/gaining further insight into the molecular mechanisms underlying  $\beta$  cell (neo)genesis during pancreas morphogenesis and throughout adulthood are of growing interest. Consequently, several studies demonstrated that during pancreatic development, the cooperation of several transcription factors successively specifies endodermal progenitor cells toward the pancreatic, endocrine, and ultimately hormone-expressing cell fates. Among the latter, *Arx* and *Pax4* mutually inhibit each other at the transcriptional

level and thereby differentially specify the  $\alpha$  and  $\beta/\delta$  cell fates, respectively (Sosa-Pineda et al., 1997; Collombat et al., 2003). Interestingly, it was shown that the ectopic expression of *Pax4*, or the specific loss of *Arx*, in adult or embryonic  $\alpha$  cells trigger their conversion into  $\beta$ -like cells and their subsequent neogenesis from the ductal epithelium (Collombat et al., 2009; Al-Hasani et al., 2013; Courtney et al., 2013). Importantly, such a cycle of neogenesis and conversion results in a high number of  $\beta$ -like cells that are functional and can revert the consequences of chemically induced diabetes multiple times. It is worth noting that in these different models, in addition to glucagon-expressing cells neogenesis, an increase in the number of somatostatin-expressing  $\delta$ -like cells was consistently observed. Unexpectedly, although continuously detected, these  $\delta$  cells were not found to accumulate over time. Based on these observations, and considering that  $\delta$  cells are closely related to  $\beta$  cells during development, we sought to determine whether adult  $\delta$  cells could not be induced to adopt a  $\beta$ -like cell identity. To address this question, we generated animals allowing the ectopic expression of *Pax4* specifically in  $\delta$  cells. Interestingly, our results provide evidence that adult  $\delta$  cells can be reprogrammed into functional  $\beta$ -like cells upon the sole expression of *Pax4*. Importantly, we show a progressive islet neogenesis and islet hypertrophy together with dramatic endocrine cell hyperplasia. Together, our

Correspondence to Patrick Collombat: collombat@unice.fr

Abbreviations used: EMT, epithelial-to-mesenchymal transition; IdU, iodo-deoxyuridine; STZ, streptozotocin.

© 2017 Druelle et al. This article is distributed under the terms of an Attribution-Noncommercial-Share Alike-No Mirror Sites license for the first six months after the publication date (see <http://www.rupress.org/terms/>). After six months it is available under a Creative Commons License [Attribution-Noncommercial-Share Alike 4.0 International license, as described at <https://creativecommons.org/licenses/by-nc-sa/4.0/>].

Supplemental material can be found at:  
<http://doi.org/10.1083/jcb.201704044>



analyses suggest that the  $\delta$ -to- $\beta$ -like cell conversion provokes a disruption of islet homeostasis triggering a reawakening of the endocrine differentiation program and resulting in a cycle of endocrine cell neogenesis and further  $\delta$ -to- $\beta$ -like cell reprogramming. Interestingly, upon chemically induced diabetes, transgenic mice ectopically expressing *Pax4* in  $\delta$  cells display an extended life span and a partial recovery of the  $\beta$  cell mass.

## Results

### Generation and characterization of animals allowing the ectopic expression of *Pax4* in somatostatin-expressing cells

Aiming to determine whether the sole ectopic expression of *Pax4* in  $\delta$  cells could alter their phenotype/identity *in vivo*, we first crossed Sst-Cre animals (Fig. 1 A) with the ROSA26- $\beta$ -gal mouse line (Soriano, 1999; Fig. 1 A). Our analyses of the pancreata from the resulting Sst-Cre::ROSA26- $\beta$ -gal transgenic mice validated the specificity of *Cre* expression solely in somatostatin-producing cells (Fig. 1 C). Importantly, no glucagon-expressing cells were found positive for the  $\beta$ -galactosidase tracer, further confirming such  $\delta$  cell specificity (Fig. 1 D). Subsequently, Sst-Cre animals were mated with *Pax4*-OE mice (Collombat et al., 2009; Fig. 1 B). In the resulting Sst-Cre::Pax4-OE double-transgenic animals, *Pax4* ectopic expression was clearly detected in *Cre*-expressing somatostatin<sup>+</sup> cells (Fig. 1, E–G). Accordingly, quantitative analyses confirmed such specificity with an ectopic expression of *Pax4* in  $66 \pm 3.09\%$  of somatostatin-expressing cells (Fig. 1, E and F). Importantly, Sst-Cre::Pax4-OE transgenic mice were found to be viable and fertile, and no premature death was observed. Along the same line, no statistical difference was observed in the glycemia of control and transgenic animals of matching ages (Fig. 1 H), demonstrating that the ectopic expression of *Pax4* in somatostatin<sup>+</sup> cells does not impact basal glycemia levels.

### *Pax4* expression in $\delta$ cells results in progressive islet hypertrophy and insulin-producing cell hyperplasia

The pancreata of Sst-Cre::Pax4-OE animals and age-/sex-matched controls were analyzed by immunofluorescence at 2, 5, and 8 mo of age. Importantly, an increase in islet number and size was evidenced in 2-mo-old Sst-Cre::Pax4-OE animals compared with controls (Fig. 2, A and B). As interesting were the further augmentations in both islet number and size observed in 5- and 8-mo-old Sst-Cre::Pax4-OE pancreata relative to controls (Fig. 2, C and D), suggestive of progressive processes. Quantitative analyses corroborated these results with the demonstration of a significant ( $2.38 \pm 0.43$ -fold) increase in islet counts and a  $1.48 \pm 0.27$ -fold augmentation in islet size when comparing 2-mo-old Sst-Cre::Pax4-OE pancreata with matched controls (Fig. 2, E and F). Importantly, the quantification of insulin<sup>+</sup> cells per pancreas demonstrated that the islet hypertrophy/multiplication mostly resulted from a significant insulin<sup>+</sup> cell hyperplasia with a  $3.43 \pm 0.09$ -fold increase in insulin<sup>+</sup> cell numbers compared with controls (Fig. 2 G). Additional analyses performed in 5-mo-old animals ascertained a further increase reaching  $3.30 \pm 0.20$ -fold in the islet count,  $2.27 \pm 0.11$ -fold in islet size, and a massive  $7.57 \pm 0.08$ -fold in insulin<sup>+</sup> cell counts as compared with controls (Fig. 2, E–G). Similar augmentations were also observed in 8-mo-old animals

when compared with age-/sex-matched controls (Fig. 2, E–G), suggestive of a plateau in islet growth and multiplication after 5 mo of age. Focusing our quantitative studies on the relative endocrine cell proportions within hypertrophic islets versus controls, the insulin<sup>+</sup> cell share was found slightly higher than normal in 5-mo-old Sst-Cre::Pax4-OE islets (Fig. 2 H), whereas the glucagon<sup>+</sup> cell proportion was unchanged (Fig. 2 I). Surprisingly, the somatostatin<sup>+</sup> cell share was  $1.61 \pm 0.65$ -fold reduced in 2-mo-old Sst-Cre::Pax4-OE islets and further diminished ( $3.05 \pm 0.53$ -fold) in their 5-mo-old counterparts (Fig. 2 J). In addition to the evidently altered endocrine cell counts observed in Sst-Cre::Pax4-OE pancreata, an abnormal positioning of non- $\beta$  cells was noted within the islets. Indeed, although glucagon- and somatostatin-expressing cells were predictably found uniformly distributed at the periphery of control islets (Fig. S1, A and B; and Video 1), a preferential localization at a pole of the islets, close to adjacent ducts, was evidenced for these non- $\beta$  cells in 2-mo-old Sst-Cre::Pax4-OE islets (Fig. S1, C and D; and Video 1). Interestingly, these alterations appeared to result from a continued endocrine cell neogenesis processes. Accordingly, quantitative analyses of the total glucagon- and somatostatin-expressing cell counts per pancreatic sections revealed a progressive increase of both cell subpopulations in the pancreas of Sst-Cre::Pax4-OE transgenics (Fig. S1, E and F). Together, these results suggest that the ectopic expression of *Pax4* in  $\delta$  cells promotes a progressive increase in islet number, size, and cell content until 5 mo of age.

### Ectopic expression of *Pax4* in somatostatin<sup>+</sup> cells induces their conversion into $\beta$ -like cells

To investigate the fate/destiny of *Pax4*-expressing  $\delta$  cells in Sst-Cre::Pax4-OE pancreata, further immunofluorescence experiments were undertaken. The expression of the  $\beta$ -galactosidase tracer was therefore monitored, comparing Sst-Cre::ROSA26- $\beta$ -gal mice with Sst-Cre::Pax4-OE animals. In Sst-Cre::ROSA26- $\beta$ -gal control pancreata,  $\beta$ -gal<sup>+</sup> cells were found, as expected, in the mantle of the islets, where somatostatin-expressing cells are normally located (Fig. 3 A). Although no insulin/ $\beta$ -gal double-positive cells could be found in control islets (Fig. 3 A), several insulin<sup>+</sup>/ $\beta$ -galactosidase<sup>+</sup> cells were detected in 2-mo-old Sst-Cre::Pax4-OE pancreata (Figs. 3 B and S2 A). Interestingly, similar lineage tracing experiments performed on 5-mo-old transgenics revealed a further increased number of insulin<sup>+</sup> cells labeled with  $\beta$ -galactosidase (Figs. 3 C and S2 B). These results were confirmed using quantitative analyses. Indeed, although no insulin<sup>+</sup> cells expressed  $\beta$ -galactosidase in control islets, a proportion of  $3.1 \pm 0.36\%$  of insulin<sup>+</sup> cells expressed  $\beta$ -galactosidase in 2-mo-old transgenic islets (Fig. 3 D). Similarly,  $5.1 \pm 0.69\%$  of insulin<sup>+</sup> cells were labeled by  $\beta$ -galactosidase in 5-mo-old transgenic islets (Fig. 3 D). To investigate the mechanisms by which *Pax4* could induce such conversion, we sought to assess the expression of several  $\delta$  cell markers (despite their low number). Interestingly, although all somatostatin-expressing cells expressed the  $\delta$  cell marker *Hhex* in control islets (Fig. 3 E), several somatostatin<sup>+</sup>/*Hhex*<sup>−</sup> cells were detected within the islets of Sst-Cre::Pax4-OE transgenics (Fig. 3 F). *Hhex* is required for  $\delta$  cell specification (Zhang et al., 2014), and *Pax4* ectopic expression appears to result in a down-regulation of *Hhex* and promotes the acquisition of a  $\beta$ -like cell phenotype. Together, these findings demonstrate that *Pax4* expression in somatostatin<sup>+</sup> cells induces their conversion

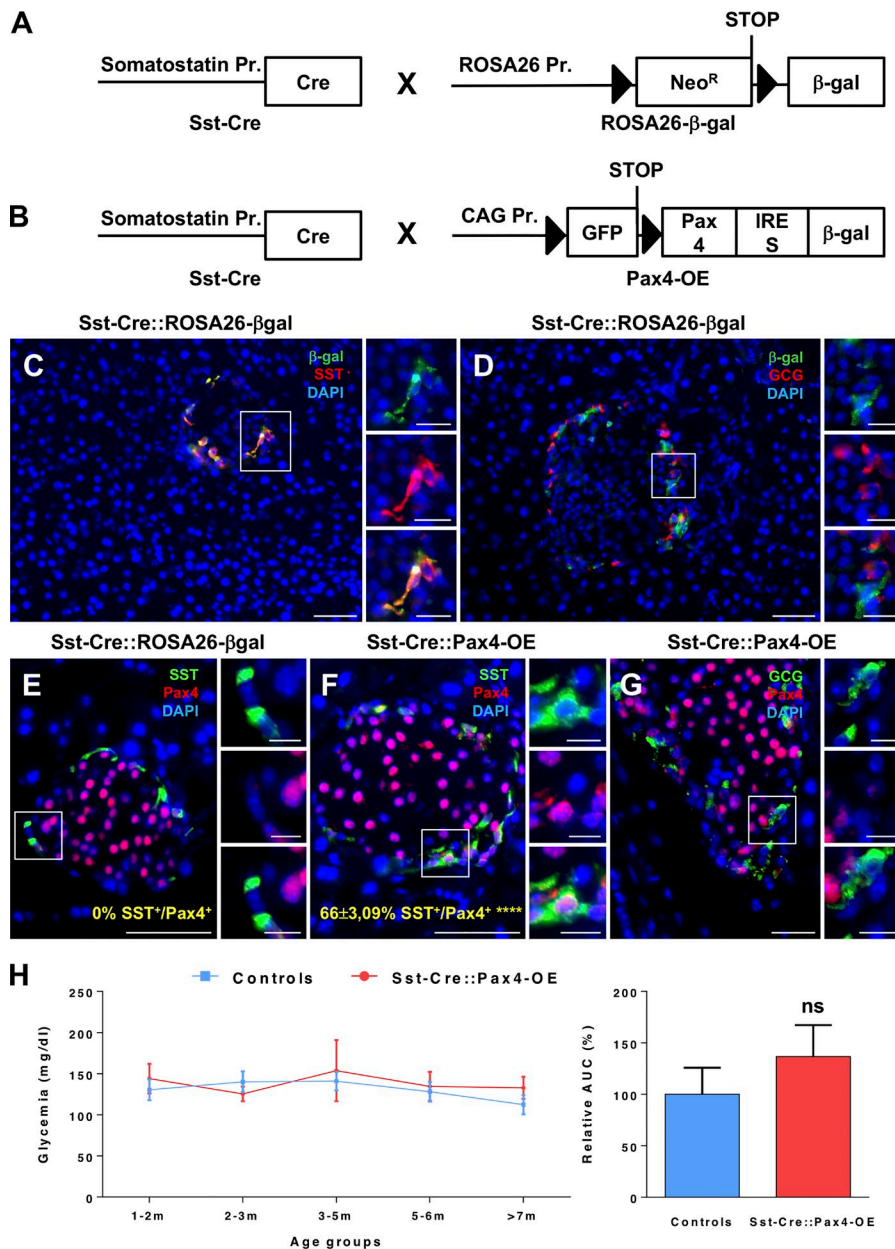


**Figure 1. Generation and validation of animals allowing *Pax4* ectopic expression in somatostatin-expressing cells.** (A and B) Control Sst-Cre::ROSA26-βgal double-transgenic mice were obtained by crossing Sst-Cre animals with the ROSA26-βgal line (in which the *Rosa26* promoter is upstream of a neomycin resistance-STOP cassette driven by *LoxP* sites and followed by the β-galactosidase reporter; A). Sst-Cre mice were also crossed with Pax4-OE animals (in which the CAG promoter is upstream of the GFP-STOP flanked by *LoxP* sites and followed by the *Pax4* and β-galactosidase cDNA sequences; B). In the resulting Sst-Cre::Pax4-OE bitransgenic mouse line, somatostatin expression drives the expression of the *Cre recombinase* and allows the excision of the region between the two *LoxP* sites thereby promoting the expression of *Pax4* and β-galactosidase (B). (C and D) β-Galactosidase and somatostatin immunodetection in Sst-Cre::ROSA26-βgal double-transgenic mice ( $n = 4$ ) confirmed *Cre* activity specifically in somatostatin-expressing cells. (E–G) In Sst-Cre::Pax4-OE islets ( $n = 4$ ), *Pax4* was detected in  $66 \pm 3.09\%$  of the somatostatin-expressing cells (E and F) and was not found in glucagon<sup>+</sup> cells (G). (H) Glycemia of nonfasted control and transgenic mice of different ages (1–2 mo,  $n = 5$ ; 2–3 mo,  $n = 16$ ; 3–5 mo,  $n = 10$ ; 5–6 mo,  $n = 6$ ; >7 mo,  $n = 5$ ). The area under the curve (AUC) was measured and demonstrated no statistical differences between both groups (H). For *Cre recombinase* efficiency, the *p*-value was calculated using a one-sample *t* test. All values are depicted as mean  $\pm$  SEM. Statistics for AUC were determined using the Mann–Whitney test. \*\*\*\*,  $P < 0.0001$ ; ns,  $P > 0.05$ . Bars: 50  $\mu$ m; (insets) 20  $\mu$ m. β-gal, β-galactosidase; GCG, glucagon; SST, somatostatin.

into β-like cells, presumably through *Hhex* inhibition. Unfortunately, further in-depth analyses are impossible because of the lack of a proper δ cell line (for in vitro studies) and the small number of such cells (for in vivo assessment). Importantly, and considering that the insulin<sup>+</sup> cell count per islet massively increases with age, our results suggest that the proportion of insulin<sup>+</sup> cells with a δ cell ontogeny increases proportionally with the islet growth. As important is the observation that most neo-generated insulin<sup>+</sup> cells are not derived from δ cells, indicating that additional processes are at play.

#### Ectopic expression of *Pax4* in δ cells results in increased proliferation within the ductal epithelium

Our results demonstrate that the ectopic expression of the *Pax4* gene in δ cells is sufficient to induce their reprogramming into cells displaying an insulin<sup>+</sup> cell identity. However, this conversion can clearly not account for the massive endocrine cell

hyperplasia observed in Sst-Cre::Pax4-OE animals, suggestive of the involvement of additional mechanisms. Thus, to investigate whether the latter could imply an increase in cell replication, cell proliferation rates were assayed in Sst-Cre::Pax4-OE mice and matched controls treated with either iodo-deoxyuridine (IdU) or BrdU for different durations. Importantly, after a short IdU pulse (3 d), a significant augmentation in replicating cell numbers was observed in the pancreas of 2-mo-old transgenics, as indicated by increased IdU<sup>+</sup> cell numbers (Fig. 4, A and E). Strikingly, most proliferating cells were located not within the islets of Langerhans but rather within the “ductal lining” (referring to cells located in the ductal epithelium and its immediate vicinity; Fig. 4 E). Aiming to monitor their outcome, pulse-chase experiments (3 d of IdU labeling followed by 7 d of chase) were performed as a means of short-term lineage tracing, as previously reported (Alcolea and Jones, 2014; Fink et al., 2015; Hsu, 2015). Importantly, after a 7-d chase, these IdU-labeled cells were found not only in the ductal lining of 2-mo-

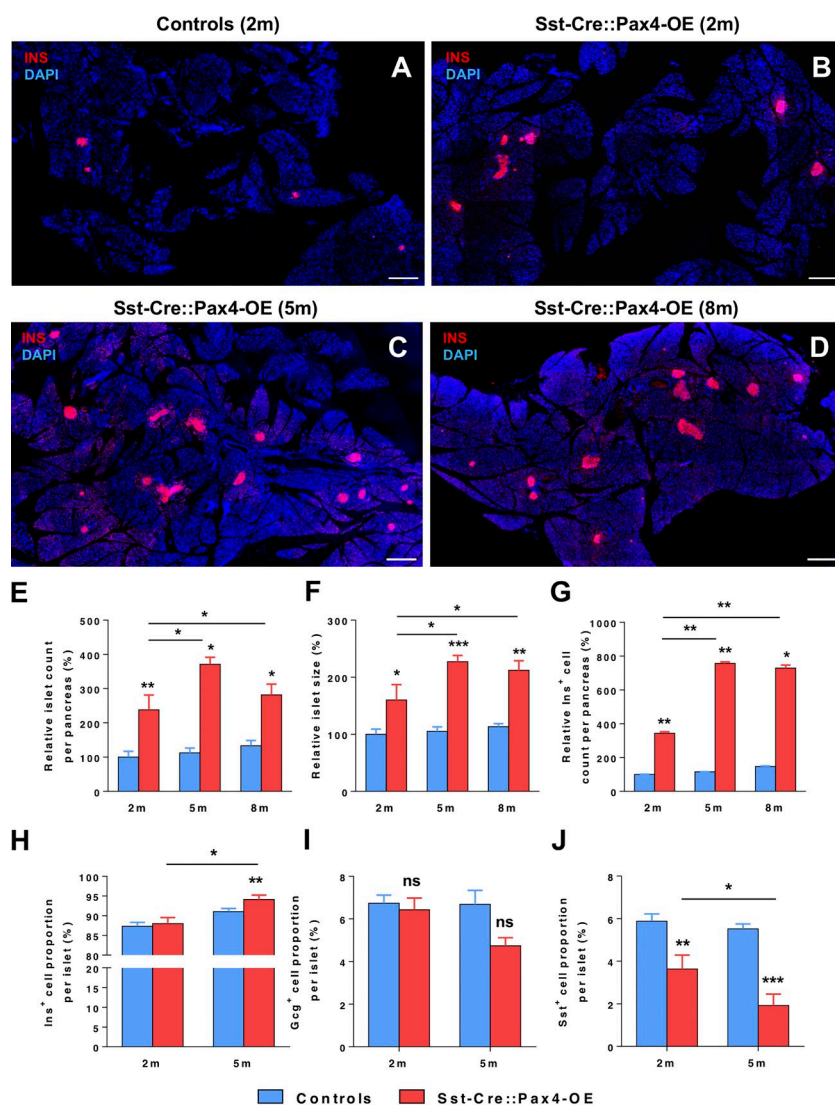


**Figure 2. The ectopic expression of Pax4 in  $\delta$  cells results in islet hypertrophy and islet neogenesis.** (A–D) Representative photographs of immunofluorescence analyses on pancreas sections of 2- (B), 5- (C), and 8-mo-old (D) transgenic and control pancreata (A) showing a dramatic increase in islet number and size. (E–J) Quantitative analyses of four animals from each group revealed an  $\sim 1.5\times$  increase in islet size (F) and an  $\sim 2\times$  increase in islet number (E) in 2-mo-old transgenic pancreata. Quantitative analyses of insulin<sup>+</sup> area in 2-mo-old mice outlined an  $\sim 4\times$  increase, consistent with the observed increase in islet number and counts (G). At 5 and 8 mo of age ( $n = 7$  and  $n = 5$ , respectively), a mean of 3 $\times$ , 2 $\times$ , and 8 $\times$  increase in islet counts (E), size (F), and insulin<sup>+</sup> area (G), respectively, was quantified in Sst-Cre::Pax4-OE pancreata as compared with age-matched controls. Quantification of insulin<sup>+</sup> cell proportions within hypertrophic islets demonstrated an increase in 2- and 5-mo-old transgenic animals ( $n = 6$ ) compared with controls ( $n = 7$ ; H). Quantification of islet glucagon<sup>+</sup> cell content in 2- and 5-mo-old mutant islets did not reveal any differences compared with controls ( $n = 7$ ; I). A significant decrease in somatostatin<sup>+</sup> proportions was observed in 2- and 5-mo-old mutant islets compared with controls ( $n = 7$ ; J). All values are depicted as mean  $\pm$  SEM. Statistics were performed with the Mann–Whitney test or unpaired *t* test with Welch’s correction. \*\*\*,  $P < 0.001$ ; \*\*,  $P < 0.01$ ; \*,  $P < 0.05$ . Bars, 500  $\mu\text{m}$ . INS/Ins, insulin.

old Sst-Cre::Pax4-OE pancreata but also within the islets of Langerhans (Fig. 4, B and F). Accordingly, longer IdU treatment (10 d) revealed numerous IdU<sup>+</sup> cells in the ductal epithelium and lining (Fig. 4, C, D, and G; and Fig. S3, A–F), and IdU<sup>+</sup> cells were also found within the islets of Sst-Cre::Pax4-OE mice (Fig. 4, C, D, and H), further suggesting that proliferating cells migrated from the ductal compartment to the islets of Langerhans. Of note, the slow rate of proliferation in control ducts was also observed in larger ducts (Fig. S3, A–C), whereas increased ductal proliferation was also detected in smaller ducts in 2-mo-old Sst-Cre::Pax4-OE transgenics (Fig. S3, D–F), indicating that the increase in the proliferation of duct-lining cells in transgenic pancreata does not seem to depend on the size of the ducts. Quantitative analyses verified these observations and outlined a  $5.73 \pm 0.38$ -fold increase in the numbers of IdU<sup>+</sup> cells solely within the ductal lining or epithelium after short-term IdU treatment comparing Sst-Cre::Pax4-OE pancreata and controls (Fig. 4 I). Chasing the label for 7 d resulted in a  $3.93 \pm 0.41$ -fold augmentation in IdU<sup>+</sup> cell counts within the endocrine compartment of 2-mo-old Sst-Cre::Pax4-OE pancreata, whereas a  $4.10 \pm 1.04$ -fold increase was still detected within the ductal lining/epithelium. Similar results were obtained after 10 d of IdU treatment with a  $2.47 \pm 0.14$ -fold increase in the numbers of IdU<sup>+</sup>

cells within the endocrine compartment (Fig. 4 I). Of note, no difference in IdU<sup>+</sup> cell counts was observed in the acinar tissue comparing both groups (Fig. 4 I). Concomitant with the plateau in islet hypertrophy observed after 5 mo of age, comparative quantifications of endocrine and nonendocrine cell proliferation rates in 5- and 8-mo-old mutants did not reveal any differences (Fig. S3 G). Thus, these data suggest that the observed augmentations in islet size and number mostly involve increased cell proliferation. Importantly, combined with the demonstration of the preferential localization of non- $\beta$  cells, these results strongly suggest that the increased cell replication essentially originate from the ductal lining/epithelium, these proliferating cells eventually migrating to the islets of Langerhans and acquiring an endocrine cell identity.

#### Reexpression of *Neurog3* and epithelial-to-mesenchymal transition (EMT) markers in Sst-Cre::Pax4-OE pancreata

Aiming to gain further insight into the mechanisms underlying ductal cell proliferation and the resulting endocrine cell neogenesis observed in Sst-Cre::Pax4-OE pancreata, we wondered whether these processes could involve a reawakening of the developmental endocrine differentiation program that would

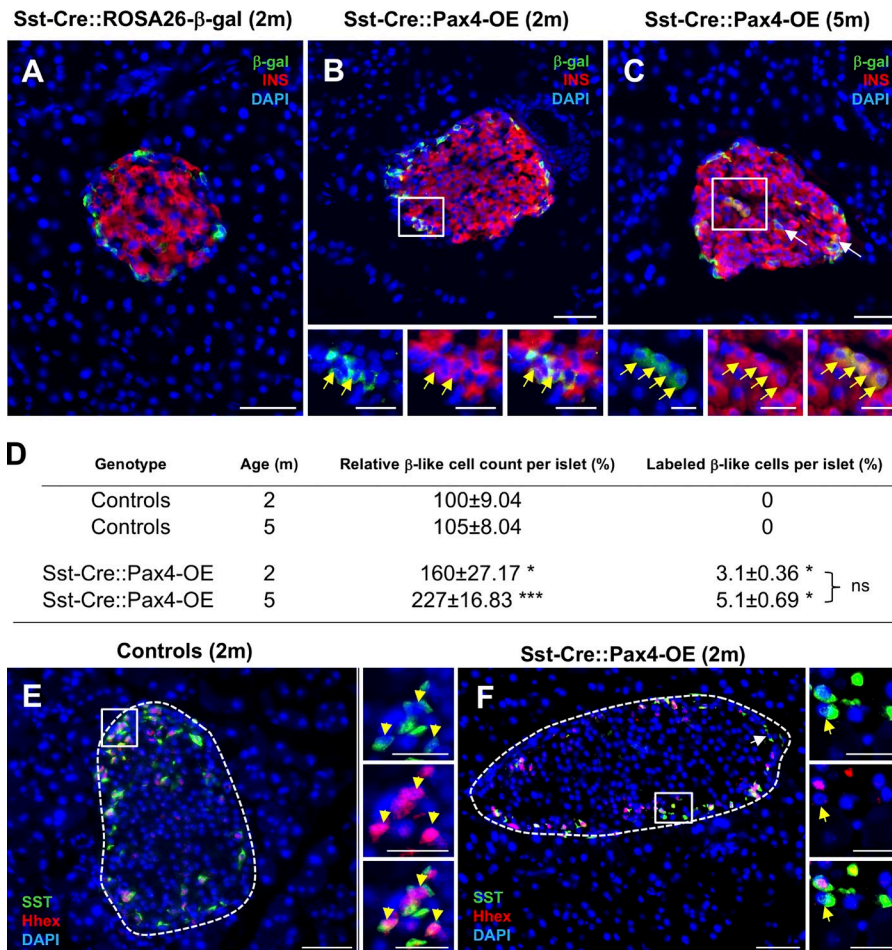
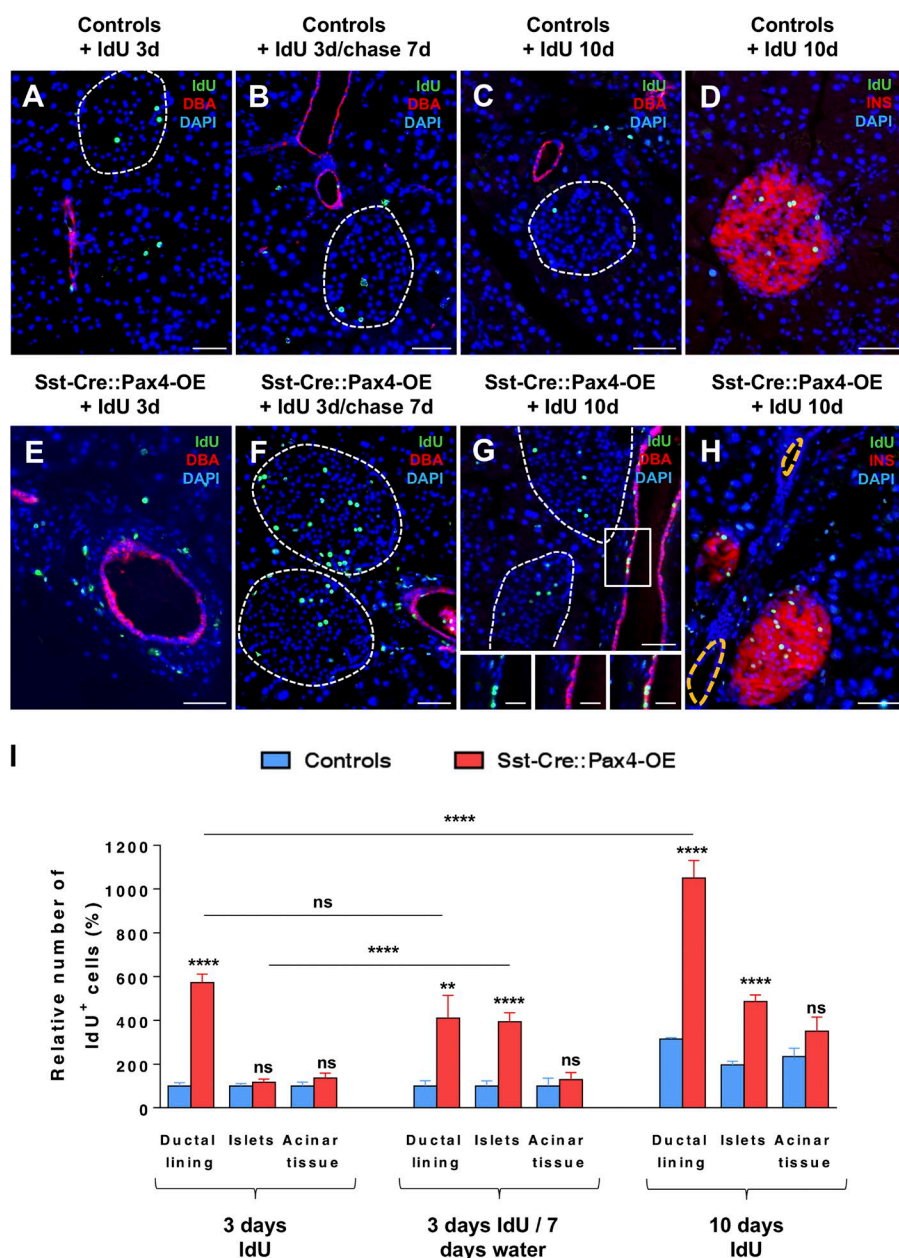


**Figure 3. Conversion of adult  $\delta$  cells into insulin-producing cells upon *Pax4* ectopic expression.** (A–C) Representative photographs of lineage tracing experiments performed on 2- and 5-mo-old pancreata ( $n = 4$ ). Although  $\beta$ -galactosidase<sup>+</sup> cells did not label insulin<sup>+</sup> cells in Sst-Cre::ROSA26- $\beta$ -gal control islets (A), immunofluorescence experiments showed several insulin<sup>+</sup> cells positive for the  $\beta$ -galactosidase tracer in Sst-Cre::Pax4-OE pancreata (B and C, insets and arrows), indicative of a conversion of  $\delta$  cells into insulin<sup>+</sup> cells. (D) Further examinations revealed that 3.1% of insulin<sup>+</sup> cells in 2-mo-old transgenics expressed  $\beta$ -galactosidase, and this proportion was maintained in 5-mo-old Sst-Cre::Pax4-OE animals. (E and F) Immunofluorescence analyses assessing *Hhex* expression in somatostatin-expressing cells in controls (E) and Sst-Cre::Pax4-OE (F) pancreata. Note the detection of somatostatin<sup>+</sup>/*Hhex*<sup>+</sup> cells solely within the islets of Sst-Cre::Pax4-OE transgenics (F, arrows in inset). For the purpose of clarity, in selected photographs, islets are outlined with dashed white lines. Statistics were determined using a Mann–Whitney test (\*\*\*,  $P < 0.001$ ; \*,  $P < 0.05$ ). Bars: 50  $\mu$ m; (insets) 20  $\mu$ m. INS, insulin; SST, somatostatin.

result in the neogenesis of all endocrine cell subtypes as seen during embryogenesis. Thus, to test this hypothesis, the expression of the proendocrine/developmental master gene *Neurog3* was investigated. Whereas *Neurog3* was expectedly not found expressed in adult control pancreas (Fig. 5 A), a reexpression of this proendocrine gene was evidenced in several ductal cells and within the ductal lining (Fig. 5 B). Because of known difficulties to detect *Neurog3* expression by immunofluorescence and to ascertain the reexpression of this proendocrine gene, total pancreas quantitative RT-PCR analyses were performed. A  $2.26 \pm 0.30$ -fold increase in *Neurog3* transcripts was demonstrated in 2-mo-old Sst-Cre::Pax4-OE pancreata, further confirming its reexpression (Fig. 5 K). Similarly, a  $3.40 \pm 1.19$ -fold increase in the expression of the *Neurog3* target *IA1* was observed (Fig. 5 K). Combined, these observations support the notion of a reawakening of the expression of *Neurog3* in the ductal lining of adult animals expressing *Pax4* in  $\delta$  cells. Importantly, *Neurog3*<sup>+</sup> cells give rise to all endocrine cells during development, further suggesting that the islet hypertrophy observed Sst-Cre::Pax4-OE could be caused by a reenactment of the developmental endocrine differentiation program. Aiming to further ascertain this hypothesis, we focused our analyses on the EMT, a key developmental process. EMT is orchestrated by a cascade of events, including the loss of an epithelial cell identity and the acquisition of a mesenchymal cell phenotype and associated markers (such as vimentin, nestin, Sox11, Snail2, and N-cadherin; Chiang and Melton, 2003). We therefore assessed the expression of an EMT hallmark, *Vimentin*, in 2-mo-

old Sst-Cre::Pax4-OE pancreata and controls. Surprisingly, our analyses revealed a massive increase in the numbers of vimentin<sup>+</sup> cells in the ductal epithelium, ductal lining, and close to adjacent islets (Fig. 5, C–J). Total pancreas quantitative RT-PCR analyses further confirmed these observations when focusing on additional EMT markers, with a 1.8-fold increase in *Snail2* transcripts, a 15-fold increase in *Nestin* expression, and an eight-fold augmentation of *Sox11* transcripts in 2-mo-old transgenic pancreata compared with controls (Fig. 5 K). To verify that no inflammation or fibrosis occurred in the pancreas of transgenic mice, hematoxylin and eosin and Sirius red colorations were performed on 2-mo-old pancreatic sections. The results obtained did not show any abnormalities, collagen deposits, or inflammatory infiltration (Fig. S4, A–D). In addition, to verify whether vimentin<sup>+</sup> cells could correspond to pancreatic stellate cells, we focused our analyses on activated stellate cell markers, such as  $\alpha$ -SMA or ICAM-I. None of these marker genes were detected in Sst-Cre::Pax4-OE pancreata, thus excluding a putative activation of pancreatic stellate cells (Fig. S4, E–H). Interestingly, further examination of Sst-Cre::Pax4-OE animals treated for 10 d with BrdU also unraveled several duct-lining BrdU<sup>+</sup> cells expressing *Vimentin* (Fig. 5, E and F), suggesting that proliferating ductal cells undergo EMT. Additional analyses of 2-mo-old transgenics and controls revealed the presence of vimentin<sup>+</sup>/synaptophysin<sup>+</sup> cells located close to ducts (Fig. 5, G and H), indicating that cells undergoing EMT adopt an endocrine cell identity. Accordingly, vimentin<sup>+</sup>/ $\beta$ -galactosidase<sup>+</sup> cells were also detected within the ductal lining of 2-mo-old



Sst-Cre::Pax4-OE transgenics (Fig. 5, I and J). Together, these results support the notion that *Pax4* ectopic expression in  $\delta$  cells eventually induces a reawakening of endocrine developmental processes with the reexpression of *Neurog3* in duct-lining cells and associated developmental processes, such cells eventually adopting an endocrine cell identity. Indeed, although ductal cell lineage tracing is impossible in the present context, the data accumulated suggest that proliferating ductal cells eventually adopt an endocrine cell identity by reenactment of the endocrine developmental program.

#### Neo-generated insulin-expressing cells in Sst-Cre::Pax4-OE pancreata display a $\beta$ cell phenotype and are functional

To further investigate the identity of the neo-generated insulin-expressing cells observed in Sst-Cre::Pax4-OE pancreata, thorough marker gene analyses were performed in 2-, 5- and 8-mo-old animals. In all three instances, our data indicated

that all insulin<sup>+</sup> cells (preexisting and neo-generated) displayed a  $\beta$ -like cell phenotype. Indeed, these cells uniformly expressed the bona fide  $\beta$  cell labels, such as *PC1/3* (Fig. 6, A–D), *Glut-2* (Fig. 6, E–H), *Nkx6.1* (Fig. 6, I–L), *Pdx1* (Fig. 6, M–P), and the pan-endocrine genes *NeuroD1* (Fig. 6, Q–T) and *Pax6* (Fig. 6, U–X). To assess the function of Sst-Cre::Pax4-OE insulin<sup>+</sup> cells, intraperitoneal glucose tolerance tests were performed on 2-mo old Sst-Cre::Pax4-OE mice and matched controls. Interestingly, transgenic mice displayed an improved response with a lower peak in glycemia and a faster return to normoglycemia than controls (Fig. 7 A), suggestive of an increased functional  $\beta$ -like cell mass. In addition, insulin tolerance tests did not revealed any significant difference between 2-mo-old Sst-Cre::Pax4-OE animals and matching controls (Fig. 7 B), indicating that despite an increased  $\beta$ -like cell content, Sst-Cre::Pax4-OE mice do not develop any insulin resistance. These analyses led us to conclude that the hyperplastic insulin-expressing cells observed after the ectopic

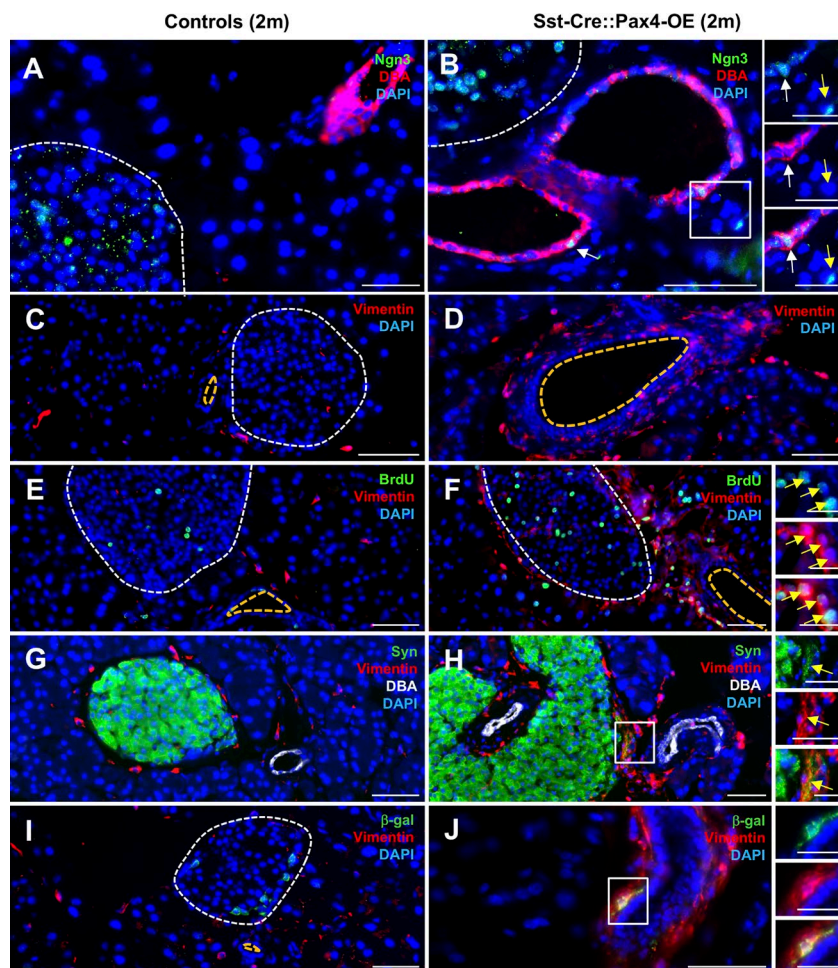


**Figure 5. Reexpression of *Neurog3* in duct-lining cells and reawakening of the EMT in *Sst-Cre::Pax4-OE* pancreata.** (A–J) Immunofluorescence experiments were performed on pancreatic sections of 2-mo-old transgenics (B, D, F, H, and J) and matched controls (A, C, E, G, and I). *Neurog3* was reexpressed in the ductal lining (B, yellow arrow) and epithelium (B, white arrow) of 2-mo-old transgenic mice but absent in matched-controls (A). Surprisingly, the mesenchymal marker *Vimentin* was largely expressed in the ductal lining epithelium of 2-mo-old transgenic animals ( $n > 5$ ; D, F, H, and J) but weakly expressed in control mice ( $n > 5$ ; C, E, G, and I), supporting the notion of an EMT reawakening after *Pax4* expression in somatostatin<sup>+</sup> cells. Moreover, *vimentin*-expressing cells labeled by BrdU were detected in *Sst-Cre::Pax4-OE* pancreata (inset in F), such cells being absent in matched controls (E). Further analyses of 2-mo-old mice revealed the presence of *vimentin*<sup>+</sup>/*synaptophysin*<sup>+</sup> cells (G and H) and *vimentin*<sup>+</sup>/*β-galactosidase*<sup>+</sup> cells (I and J) located close to adjacent ducts in transgenics. (K) Quantitative RT-PCR analyses confirmed our results with a mean  $2.26 \pm 0.30$ -fold increase in *Neurog3* transcripts ( $n = 4$ ) as well as an increase of 240% and 81% in the expression of *IA1* and *Snail2*, respectively ( $n = 4$ ). Further analyses revealed massive augmentations of *Nestin* and *Sox11* expression in 2-mo-old transgenic pancreata (K). All values are depicted as mean  $\pm$  SEM of  $n = 3$  independent animals. Statistical analyses were performed with the Mann–Whitney test (\*\*,  $P < 0.01$ ; \*,  $P < 0.05$ ). For the purpose of clarity, in selected photographs, islets are outlined with dashed white lines and the ductal lumen with dashed yellow lines. Bars: 50  $\mu$ m; (insets) 20  $\mu$ m. DBA, dolichos biflorus agglutinin; Syn, synaptophysin.

**K**

Genes	Controls (2m)	<i>Sst-Cre::Pax4-OE</i> (2m)
<i>Neurog3</i>	100 $\pm$ 39	226.92 $\pm$ 30.54 * (+126.92%)
<i>IA1</i>	100 $\pm$ 27	340.20 $\pm$ 119.20 * (+240.20%)
<i>Snail2</i>	100 $\pm$ 16	181.80 $\pm$ 23.40 * (+81.80%)
<i>Nestin</i>	100 $\pm$ 3.15	1544.67 $\pm$ 310.28 * (+1444.67%)
<i>Sox11</i>	100 $\pm$ 38.9	808.44 $\pm$ 202.20 * (+708.44%)

expression of *Pax4* in somatostatin<sup>+</sup> cells exhibit a  $\beta$ -like cell phenotype and are functional.

#### $\beta$ -like cell neogenesis in *Sst-Cre::Pax4-OE* animals subjected to $\beta$ cell ablation

The neo-generated  $\beta$ -like cells observed in *Sst-Cre::Pax4-OE* pancreata were further investigated in the context of chemically induced  $\beta$  cell ablation (Fig. 8 A). A single dose of 115 mg/kg streptozotocin (STZ) was administered to 2.5-mo-old transgenics and matching controls to induce the destruction of a vast majority of  $\beta$  cells without complete ablation to avoid predictable death (Fig. 8, B and E). As expected, after specific  $\beta$  cell loss, control and *Sst-Cre::Pax4-OE* mice developed hyperglycemia within 1 wk after injection (Fig. 8 H). Three months after injection, all control mice showed a glycemia  $>600$  mg/dl and a high rate of lethality (41%), whereas transgenic mice displayed an average glycemia of 350 mg/dl (Fig. 8 H), suggesting a partial  $\beta$  cell mass restoration and an extended life span. This was further supported by the detection of insulin-expressing cells in islets of control and transgenic mice at different times after STZ-mediated  $\beta$  cell ablation. Indeed, although

after 1 wk of STZ administration, control and *Sst-Cre::Pax4-OE* animals displayed a massive loss of insulin-expressing cells (Fig. 8, B and E), a progressive restoration of such cells was observed in transgenic mice (Fig. 8, F and G), and this partial recovery was absent in controls (Fig. 8, C and D). To further assess these regeneration processes, the  $\beta$  cell mass was quantified in control and transgenic pancreata 3 mo after STZ administration. Although decreased compared with their noninjected counterparts, STZ-treated *Sst-Cre::Pax4-OE* islets exhibited  $16 \pm 3.40\%$  insulin-expressing cells compared with  $8 \pm 1.77\%$  in treated-control islets (Fig. 8 I). Lineage tracing experiments were performed on STZ-injected control and transgenics, and we thereby detected insulin<sup>+</sup>/*β-galactosidase*<sup>+</sup> cells in *Sst-Cre::Pax4-OE* islets 3 mo after  $\beta$  cell mass ablation (Fig. 8, J and K). To get more insight into the mechanisms involved in this partial  $\beta$  cell mass restoration, we assessed the expression of the mesenchymal marker vimentin. Interestingly, an important augmentation in the number of vimentin-expressing cells was observed in *Sst-Cre::Pax4-OE* transgenics 1 mo after STZ administration when compared with matched-controls (Fig. S5, A–F). In addition, we detected synaptophysin<sup>+</sup> cells close to the

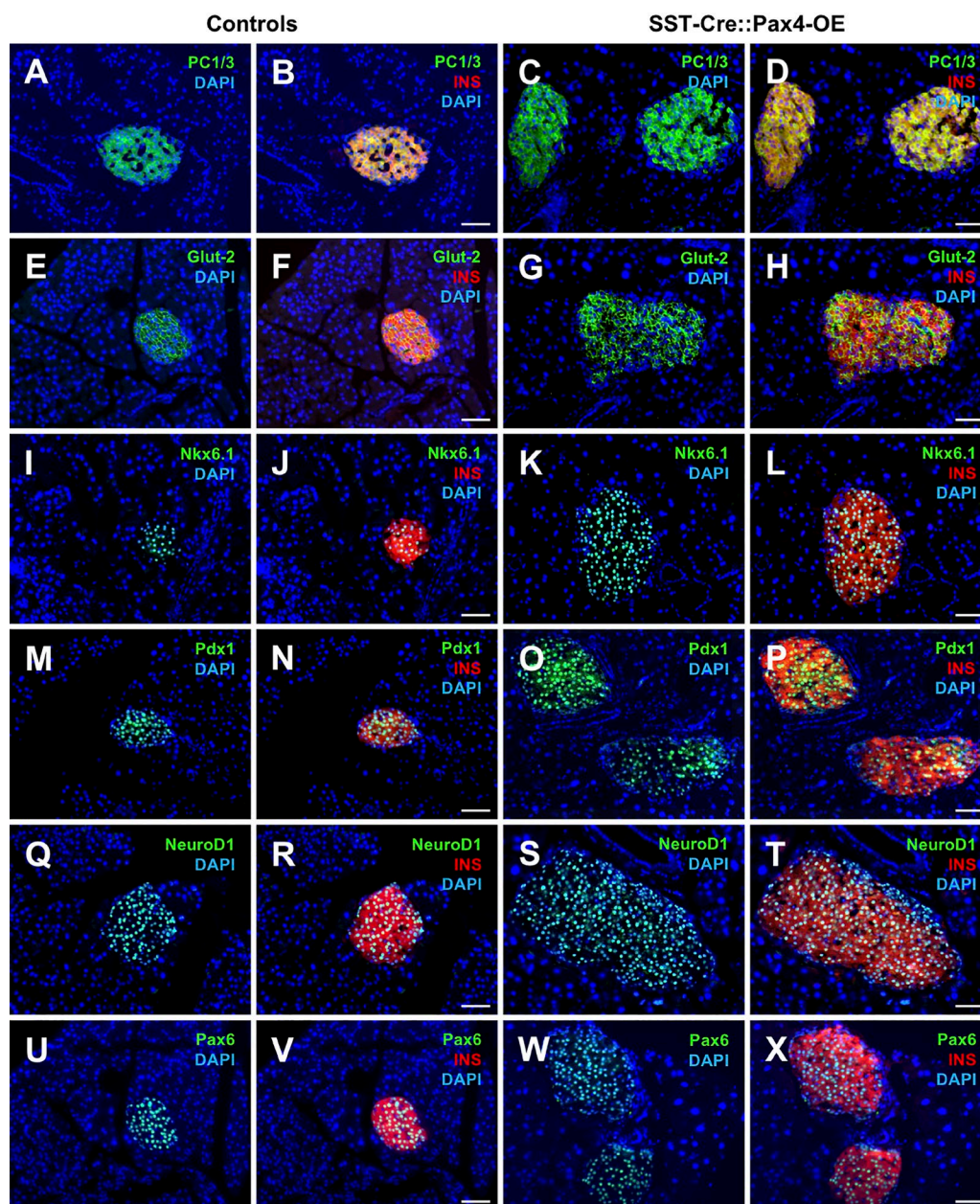
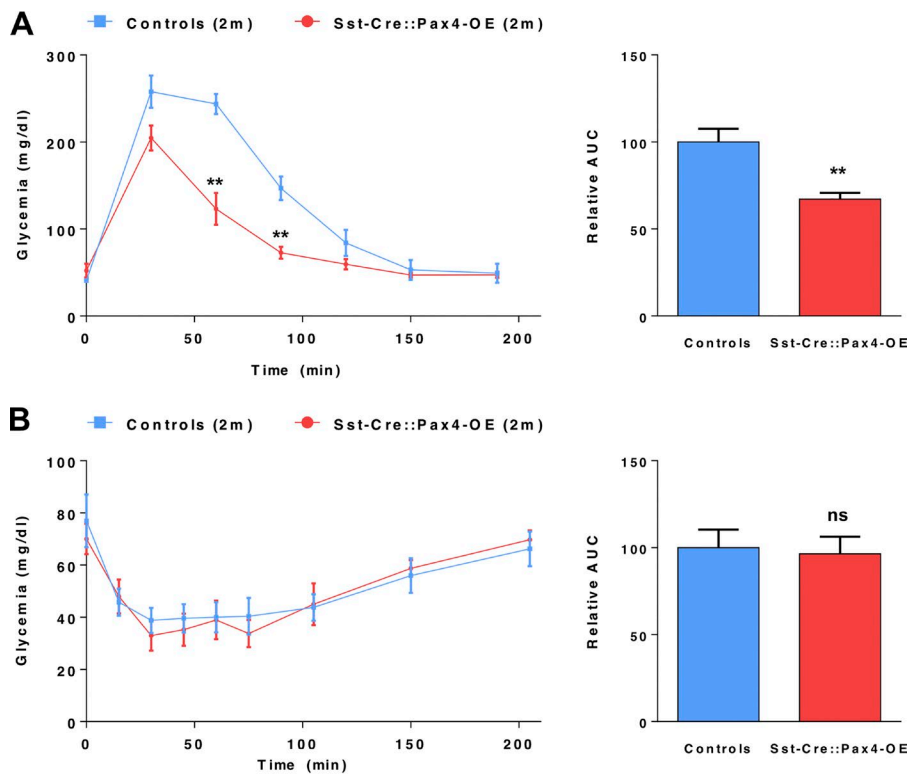


Figure 6. **Sst-Cre::Pax4OE endogenous and supplementary insulin<sup>+</sup> cells express a bona fide  $\beta$  cell-specific transcription factor complement.** Representative photographs of immunofluorescence analyses on pancreatic sections of controls ( $n > 5$ ; A, B, E, F, I, J, M, N, Q, R, U, and V) and Sst-Cre::Pax4-OE ( $n > 5$ ; C, D, G, H, K, L, O, P, S, T, W, and X). All insulin<sup>+</sup> cells (preexisting and neo-generated) uniformly expressed the bona fide  $\beta$  cell markers *PC1/3* (A–D), *Glut-2* (E–H), *Nkx6.1* (I–L), and *Pdx1* (M–P) and the pan-endocrine markers *NeuroD1* (Q–T) and *Pax6* (U–X). Bars, 50  $\mu$ m. INS, insulin.

ductal epithelium of STZ-injected Sst-Cre::Pax4-OE, and some of these cells expressed vimentin (Fig. S5, C and D). Of note, the assessment of cell proliferation after  $\beta$  cell ablation by the detection of Ki-67 protein did not reveal any difference in the number of replicating cells in the endocrine compartment when comparing controls and transgenic mice (Fig. S5, E and F), thereby excluding an increase in islet cell proliferation. Together, these results demonstrate that  $\delta$  cells can be converted into functional  $\beta$ -like cells, and such conversion results in compensatory developmental endocrine cell neogenesis. Importantly, the  $\beta$ -like cells thereby generated can partly reverse the consequences of chemically induced diabetes, resulting in an extended life span.

## Discussion

Here, we report that the ectopic expression of *Pax4* in  $\delta$  cells induces their conversion into cells displaying a  $\beta$  cell phenotype, and this induces compensatory mechanisms involving the mobilization of putative duct-lining cells that reenact developmental processes before differentiation into endocrine cells. Importantly, this cycle of neogenesis and further  $\delta$ -to- $\beta$ -like cell reprogramming results in a massive and progressive increase in the number of insulin-producing cells, resulting in islet hypertrophy and improved glucose tolerance. Equally important was the finding that neo-generated  $\beta$ -like cells are functional



**Figure 7. Improved  $\beta$  cell function in transgenic Sst-Cre::Pax4-OE mice.** (A) 2-mo-old transgenic and controls were challenged with glucose (intraperitoneal glucose tolerance tests). Strikingly, transgenic mice displayed an improved glucose clearance with a lower peak in glycemia and a faster recovery to euglycemia. The relative area under the curve (AUC) confirmed this improved glucose tolerance in 2 mo-old Sst-Cre::Pax4-OE animals. (B) Upon insulin tolerance tests (ITTs), glycemia levels of 2-mo-old transgenic and matched controls were monitored. Transgenic mice exhibited unaltered glycemia levels indicative of a normal insulin sensitivity. AUC were indeed similar in both groups. The relative AUC values are expressed as a percentage relative to the mean AUC of the controls. All values are depicted as mean  $\pm$  SEM of  $n = 5$  independent animals. Statistical analyses were performed using the Mann-Whitney test (\*\*,  $P < 0.01$ ; \*,  $P < 0.05$ ; ns,  $P > 0.05$ ).

and able to partly replace their endogenous counterparts upon chemically induced diabetes.

#### The ectopic expression of *Pax4* in $\delta$ cells induces their conversion into $\beta$ -like cells

Our results demonstrate that the ectopic expression of *Pax4* in  $\delta$  cells is sufficient to induce their efficient conversion into  $\beta$ -like cells. Indeed, we show that 3–5% of insulin<sup>+</sup> cells arise from  $\delta$  cells in 2- and 5-mo-old Sst-Cre::Pax4-OE animals (displaying a progressing insulin<sup>+</sup> cell hyperplasia), suggesting a continuous processes of  $\delta$  cell neogenesis and conversion into insulin<sup>+</sup> cells. According to a previous study, near-total  $\beta$  cell ablation in mice results in the conversion of pancreatic  $\delta$  cells into insulin-producing cells, and this conversion occurs only in juveniles (before 2 mo of age; Chera et al., 2014). Here, we demonstrate that upon *Pax4* expression, somatostatin-expressing cells retain the ability to be converted into  $\beta$ -like cells until at least 5 mo of age. Whether this arrest is caused by a loss in  $\delta$  cell plasticity or a negative feedback loop controlling the total endocrine cell content would require the establishment of an inducible system. In addition, we provide evidence that the conversion of  $\delta$  cells into  $\beta$ -like cells can trigger a massive endocrine cell neogenesis, with most of these newly formed cells not displaying a  $\delta$  cell ontogeny. Furthermore, although the presence of somatostatin<sup>+</sup>/Hhex<sup>-</sup> cells within transgenic islets provides exciting insights into the mechanism by which *Pax4* induces the conversion of somatostatin-expressing cells, it is impossible to know whether *Hhex* expression is down-regulated as a consequence of *Pax4* ectopic expression or the  $\delta$ -to- $\beta$ -like cell conversion. It is indeed important to keep in mind that  $\delta$  cells are continuously regenerated and turned into  $\beta$ -like cells in Sst-Cre::Pax4-OE mice that are less than 5 mo of age. One could bypass these concerns using a  $\delta$  cell line in which *Pax4* expression is forced. However, to the best of our knowledge, there is no  $\delta$  cell line solely

expressing the somatostatin hormone, not counting the fact that cell lines rarely retain their in vivo plasticity. The generation and analysis of gain-of-function/loss-of-function mutant animals for *Hhex* or the generation and analysis of animals expressing *Pax4* in a conditional and inducible fashion in  $\delta$  cells represent interesting alternatives.

#### Recruitment of *Neurog3*-reexpressing ductal cells and EMT reawakening

In this study, we demonstrate that most neo-generated  $\beta$ -like cells are not derived from  $\delta$  cells. In fact, our analyses indicate that the  $\delta$ -to- $\beta$ -like cell conversion triggers compensatory mechanisms involving an increased proliferation of duct-lining cells, and such cells eventually adopt an endocrine cell identity. Accordingly, we outline a reexpression of the developmental gene *Neurog3* within or close to the ductal lining upon the ectopic expression of *Pax4* in somatostatin-expressing cells. Although lineage tracing of ductal cells would undeniably demonstrate the ductal ontogeny of the endocrine cell neogenesis observed in Sst-Cre::Pax4-OE animals, one may easily comprehend that it is impossible in the present context, as these transgenic animals already harbor a *Cre recombinase*-containing transgene. Indeed, to the best of our knowledge, the only available or working mouse lines allowing the lineage tracing of *Ngn3*- or *vimentin*-expressing cells rely on the Cre-Lox approach. Because of this technical limitation, we therefore resorted to short-term tracing of proliferating ductal cells combined to immunofluorescence detection of *Ngn3* (and EMT makers) and quantitative PCR assessment of *Ngn3* (and EMT makers). It is worth noting that this approach has been successfully used by others (Alcolea and Jones, 2014; Fink et al., 2015; Hsu, 2015), and adult *Neurog3*-reexpressing cells have been repeatedly described as endocrine progenitors involved in  $\beta$  cell regeneration (Xu et al., 2008; Al-Hasani et al., 2013; Pan et al., 2013). In addition,

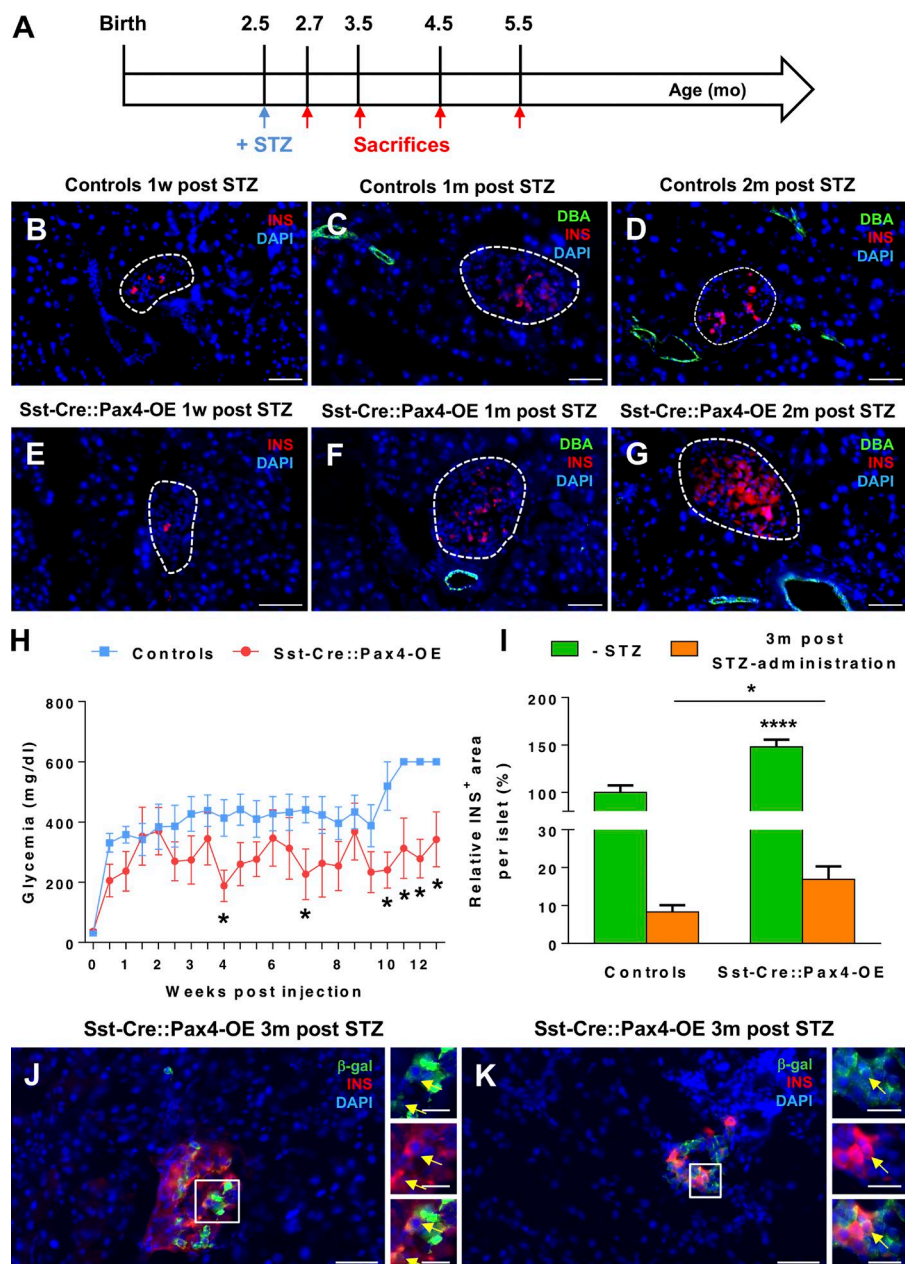


**Figure 8. The ectopic expression of Pax4 in  $\delta$  cells can induce functional  $\beta$ -like cell neogenesis upon chemically induced  $\beta$  cell ablation.** 2.5-mo-old mice were treated with STZ and sacrificed at different time points (A). Immunofluorescence assessment of insulin-expressing cells in control (B–D) or transgenic (E–G) islets outline a progressive recovery of the  $\beta$  cell mass. Monitoring of the glycemia revealed an expected peak in glycemic levels in both control and transgenic mice (H). However, 2.5 mo after  $\beta$  cell ablation, Sst-Cre::Pax4-OE mice displayed lowered glycemic levels, whereas control animals remained hyperglycemic (many of these mice died during the course of the monitoring). Quantitative analyses indicated an approximate doubling in the  $\beta$  cell area in transgenic islets 3 mo after STZ administration (I). Lineage tracing experiments of somatostatin-expressing cells performed on pancreas sections of STZ-treated mice showing  $\beta$ -gal<sup>+</sup>/insulin<sup>+</sup> cells in transgenic islets (J and K, arrows). For the purpose of clarity, in selected photographs, islets are outlined with dashed white lines. All values are depicted as mean  $\pm$  SEM of  $n = 6$  and  $n = 4$  independent control and transgenic animals, respectively. Statistical analyses were performed using the Mann–Whitney test and multiple  $t$  tests (\*\*\*\*,  $P < 0.0001$ ; \*,  $P < 0.05$ ). Bars: 50  $\mu$ m; (insets) 20  $\mu$ m. INS, insulin.

and emphasizing that *Neurog3* is responsible for the specification of all the endocrine cell lineages following specific ratios, the generation of endocrine cell types from the adult ductal epithelium would be expected to respect the standard endocrine proportions (~80% of  $\beta$  cells/~10% of  $\alpha$  cells/~10% of  $\delta$  cells). Moreover, it has been shown that during mouse pancreas morphogenesis, *Neurog3* induces the delamination of progenitor cells from the ductal epithelium through EMT processes (Gouzi et al., 2011). Interestingly, our data outline a massive increase in the expression of mesenchymal markers in the ductal lining of Sst-Cre::Pax4-OE transgenics, further supporting the idea that endocrine cell neogenesis putatively originates from the ductal epithelium. Altogether, our results clearly suggest that *Pax4* expression in  $\delta$  cells induces their conversion into  $\beta$ -like cells, subsequently activating a cycle of endocrine cell neogenesis, with the neo-generated  $\delta$  cells being yet again converted into  $\beta$ -like cells (Fig. 9).

### Partial restoration of the $\beta$ cell mass upon $\beta$ cell ablation

The ectopic expression of *Pax4* in  $\delta$  cells induces  $\beta$ -like cell neogenesis after chemically induced  $\beta$  cell ablation, resulting in a partial  $\beta$  cell mass restoration. Although not exhibiting euglycemia, Sst-Cre::Pax4-OE transgenics displayed a maximal glycemia of ~350 mg/dl and an extended life span compared with controls. The reason underlying this incomplete recovery remains unclear but could potentially involve a slow regeneration processes or a loss of  $\delta$  cell plasticity with ageing. Supporting the latter, the analyses of Sst-Cre::Pax4-OE animals suggest that  $\delta$  cells eventually lose their plasticity at ~5 mo of age. Obviously, it would be extremely interesting to determine whether such loss of regeneration potential is truly age dependent or the result of the continued endocrine neogenesis observed in Sst-Cre::Pax4-OE transgenics. The answer to this question will unfortunately have to wait for the generation of transgenic mice allowing the inducible expression of the *Cre*

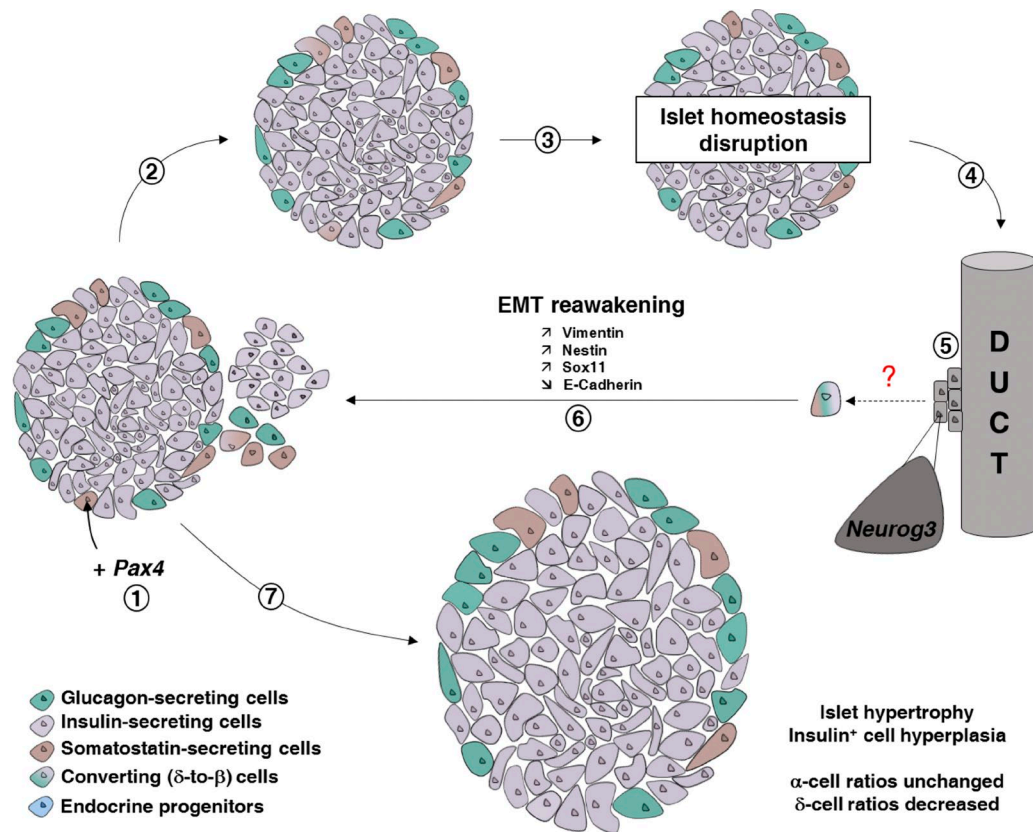


Figure 9. **Schematic illustrating the consequences of *Pax4* ectopic expression in somatostatin-expressing  $\delta$  cells.** Upon *Pax4* expression in  $\delta$  cells (1), these cells are converted into  $\beta$ -like cells (2 and 3). This leads to a disruption of islet homeostasis, mainly because of a local somatostatin shortage, further inducing the mobilization of ductal precursor cells (4), with such precursors reexpressing the proendocrine gene *Neurog3* (5). The latter cells undergo EMT before giving rise to insulin<sup>+</sup>, glucagon<sup>+</sup>, and somatostatin<sup>+</sup> cells in normal/developmental proportions (6), and neogenerated somatostatin<sup>+</sup> cells are yet again converted into  $\beta$ -like cells. Such a continuous cycle of regeneration and conversion results in insulin<sup>+</sup> cell hyperplasia, islet hypertrophy, and islet neogenesis (7).

*recombinase* in somatostatin-producing cells. Based on these findings, we suggest that the modulation of *Pax4* and/or its molecular targets could open new avenues for the treatment of diabetes and improve strategies aiming to differentiate  $\beta$ -like cells from stem, progenitor, or other types of cells.

## Materials and methods

### Ethics statement

Animal protocols were reviewed and approved by an institutional ethics committee (Ciepal-Azur) at the University of Nice, and all colonies were maintained following European animal research guidelines. This project received approval from our local ethics committee (NCE/2011-22).

### Animal procedures

Experiments were performed on transgenic and control males only. Controls included wild-type mice or transgene-negative littermates. To assess cellular proliferation, animals were treated with BrdU or IdU in the drinking water for 3 or 10 d before examination (1 mg/ml solution). All mice were housed on a standard 12:12-h light/dark cycle, with standard diet food and water ad libitum.

### Generation of the *Sst::Cre-Pax4-OE* transgenic line

Using the Cre-LoxP system to investigate  $\delta$  cell plasticity in pancreatic islets, *Sst::Cre::Pax4-OE* animals were obtained by crossing the

*Sst::Cre* mouse line (harboring a transgene encompassing the *somatostatin* promoter driving the expression of the phage P1 *Cre recombinase*; Taniguchi et al., 2011) with the previously described *Pax4-OE* line (whose transgene encompasses the ubiquitous CAG promoter upstream of a “GFP-STOP” cassette flanked by LoxP sites and followed by the *Pax4* cDNA in front of an IRES and the  $\beta$ -galactosidase reporter (Collombat et al., 2009). In the resulting bitransgenic line, *Pax4* is ectopically overexpressed in somatostatin-expressing cells and lineage of these cells can be traced.

### Histology and immunofluorescence

Tissues were fixed in 4% paraformaldehyde for 30 min at 4°C, embedded in paraffin and 8  $\mu$ m sections applied to glass slides. These sections were assayed as described previously (Collombat et al., 2003) using DAPI as counterstain. The primary antibodies used were guinea pig anti-insulin (1/500; DAKO), anti-Pdx1 (1/1,000; provided by C. Wright, Vanderbilt University, Nashville, TN); chicken anti-vimentin (1/4,000; Millipore); rat anti-somatostatin (1/250; Millipore) and anti-BrdU (1/50; Abcam); goat anti-somatostatin (1/500; Santa Cruz); mouse anti-BrdU (1/50; Roche), anti-Ngn3 (1/250; DSHB), and anti-glucagon (1/500; Sigma); rabbit anti-glucagon (1/500; R&D Systems), anti-glut-2 (1/500; Chemicon), anti-PC1/3 (1/500; Millipore), anti-Nkx6.1 (1/3000; NovoNordisk), anti-Pax6 (1/500; BioLegend), anti-Pax4 (1/500; provided by B. Sosa-Pineda, Northwestern University, Evanston, IL), anti-NeuroD1 (1/500; Millipore), and anti-synaptophysin (1/400; Abcam). The secondary antibodies (1/1,000; Invitrogen and

Jackson ImmunoResearch) used were Alexa Fluor 488, 594, and 647 and Cy3 and Cy5. For histological analyses, sections were subjected to hematoxylin and eosin or Picro-Sirius red staining. Images were processed as described in Microscope image acquisition.

#### **$\beta$ -Galactosidase-based lineage-tracing experiments**

Pancreatic tissues were isolated and fixed for 30 min at 4°C in a solution containing 1% formaldehyde, 0.2% glutaraldehyde, and 0.02% NP-40 and washed three times in cold PBS. The tissues were dehydrated in PBS-25% sucrose overnight at 4°C. Tissues were washed 2 h in Jung freezing medium (Leica Biosystems) and embedded in freezing medium on dry ice. 12- to 16- $\mu$ m sections were applied to glass slides, dried, and washed three times in PBS. After 45-min blocking in PBS-FCS 5%, sections were incubated with a rabbit anti- $\beta$ -galactosidase primary antibody (1/8,000; MP-Cappel).

#### **Microscope image acquisition**

For immunofluorescence analyses, images were collected at room temperature on an AxioImagerZ.1 upright microscope (Zeiss) equipped with a Zeiss 10 $\times$  Plan-Neofluar dry NA 0.3 and/or Zeiss 20 $\times$  Plan-Apochromat dry NA 0.8 and/or Zeiss 20 $\times$  Plan-Neofluar dry NA 0.5, a DAPI filter (excitation [Ex] 365/12 nm, dichroic mirror [DM] 395 nm, emission [Em] 445/50), a GFP filter (Ex 470/40 nm, DM 495 nm, and Em 525/50 nm), a rhodamine filter (Ex 546/12 nm, DM 560 nm, and Em 608/65 nm), a Texas red filter (Ex 560/40 nm, DM 582 nm, and Em 630/785 nm), and/or a Cy5 filter (Ex 640/30 nm, DM 660 nm, Em 690/50 nm). For mosaic acquisitions, the microscope was equipped with an automated xy stage (Märzhäuser). Images were acquired with a monochrome MRm axiocam camera (Zeiss) controlled with Axiovision 4.9.1 software (Zeiss). Posttreatment image acquisition and analysis were performed using a homemade macro on Fiji (Schindelin et al., 2012). For histological analyses, images were collected at room temperature on an AxioPlan2 upright microscope (Zeiss) equipped with a Zeiss 10 $\times$  Plan-Neofluar PH1 dry NA 0.3 objective lens. Images were acquired with a color Infinity3-6 camera (Lumenera Corporation) controlled with Micro-Manager 1.48 software (Edelstein et al., 2014).

#### **Tolerance tests and blood glucose level measurements**

For challenge purposes, animals were fasted for 16–18 h and injected intraperitoneally with 2 g/kg body weight glucose or 0.75 U/kg insulin. Blood glucose levels were measured at the indicated time points postinjection with a ONETOUCH Vita glucometer (Life Scan, Inc.).

#### **Induction of STZ-mediated diabetes**

To induce hyperglycemia, STZ (Sigma) was dissolved in 0.1 M sodium citrate buffer, pH 4.5, and a single 115-mg/kg dose was administered intraperitoneally within 10 min of dissolution. Diabetes progression was assessed by monitoring the blood glucose levels and/or survival rates of mice.

#### **RNA analyses**

Mice were euthanized by cervical dislocation and the pancreatic tissue was isolated and placed in cold RNA lysis solution (Thermo Fisher Scientific) for 48 h at 4°C. RNA was isolated (RNAeasy; QIAGEN), and cDNA synthesis (SuperScript choice system; Invitrogen) was performed according to the manufacturer's instructions. Quantitative RT-PCR was performed using validated primers (QIAGEN) and the QuantiTect SYBR Green RT-PCR kit (QIAGEN) following the manufacturer's instructions. PCR reactions and detection were performed on a Mastercycler ep realplex cyler using GAPDH as an internal control for normalization purposes.

#### **Quantifications analyses**

The entire pancreata of at least three mice per genotype and per condition were serially cut in 8- $\mu$ m-thick sections and applied to glass slides, and every 5–10 pancreatic sections were processed for immunofluorescence. For Cre recombinase efficiency and  $\beta$ -galactosidase-expressing cells, positive cells were counted manually. IdU and BrdU counting was assessed manually by counting proliferative cells in the different pancreatic compartments. Images were processed as described in Microscope image acquisition. For hormone quantifications, widefield multichannel tile scan image treatment and analysis were done using Fiji (Schindelin et al., 2012) and a homemade semiautomated macro. In brief, the overall pancreas slice area was determined and measured using a low-intensity-based threshold on hormone labeling channel. Islets were then segmented and counted on the insulin labeling, applying a high-intensity threshold. In a second step, the respective area of each segmented islet was measured. The corresponding contours were then transferred to the somatostatin or glucagon images. Finally, the signal coverage of either glucagon or somatostatin was measured and then normalized to the total area of the corresponding islet.

#### **Data analysis**

All values are depicted as mean  $\pm$  SEM of data from at least three animals. Data were analyzed using GraphPrism 6 software. Normality was tested using a D'Agostino–Pearson omnibus normality test, and appropriate statistical tests were performed. Results are considered significant if  $P < 0.0001$  (\*\*\*\*),  $P < 0.001$  (\*\*\*),  $P < 0.01$  (\*\*), and  $P < 0.05$  (\*).

#### **Online supplemental material**

Fig. S1 shows that the ectopic expression of Pax4 in  $\delta$  cells results in endocrine cell neogenesis and an abnormal positioning of non- $\beta$  cells within the islets of Sst-Cre::Pax4-OE transgenic mice. Fig. S2 shows some additional examples illustrating the conversion of  $\delta$  cells into insulin-producing cells upon Pax4 ectopic expression. Fig. S3 provides additional examples illustrating the increased proliferation of cells located within the ductal epithelium of Sst-Cre::Pax4-OE pancreata, with such augmentation occurring before 5 mo of age. Fig. S4 shows the ectopic expression of Pax4 in somatostatin-expressing cells does not induce inflammation, fibrosis, or pancreatic stellate cell activation. Fig. S5 includes further analyses of Sst-Cre::Pax4-OE mice treated with STZ. Video 1 shows islet hyperplasia and preferential localization of glucagon- and somatostatin-producing cells close to adjacent ducts.

#### **Acknowledgments**

We thank Sébastien Schaub and Maéva Gesson from the PRISM imaging platform and Samah Rekima from the Experimental Histology Platform for their help and expertise.

The authors are supported by the Juvenile Diabetes Research Foundation (C1-1-SRA-2018-536-M-R, 3-SRA-2014-282-Q-R, 3-SRA-2017-415-S-B, 2-SRA-2017-416-S-B, and 17-2013-426), the Institut National de la Santé et de la Recherche Médicale AVENIR program, the Institut National de la Santé et de la Recherche Médicale, the European Research Council (StG-2011-281265), the Fondation pour la Recherche Médicale (DRC20091217179), the Agence Nationale de la Recherche (2009 GENO 105 01/01KU0906, ANR-17-ERC2-0004-01, ANR-16-CE18-0005-02, and Betaplasticity), the "Investments for the Future" LABEX SIGNALIFE (ANR-11-LABX-0028-01), Club Isatis, Mr. and Mrs. Dorato, Mr. and Mrs. Peter de Marffy-Mantuano, the Dujean family, the Fondation Générale de Santé, and the Fondation Schlumberger pour l'Education et la Recherche.

The authors declare no competing financial interests.

Author contributions: Conceptualization, P. Collombat; Methodology, N. Druelle and P. Collombat; Software, M. Mondin; Validation, N. Druelle; Formal Analysis, N. Druelle; Investigation, N. Druelle, A. Vieira, A. Shabro, M. Courtney, M. Mondin, S. Rekima, T. Napolitano, S. Silvano, S. Navarro-Sanz, B. Hadzic, and F. Avolio; Writing – Original Draft, N. Druelle; Writing – Review and Editing, A. Mansouri and P. Collombat; Visualization, N. Druelle; Project Administration, N. Druelle and P. Collombat; Supervision, P. Collombat; Funding acquisition, P. Collombat.

Submitted: 10 April 2017

Revised: 28 July 2017

Accepted: 8 September 2017

## References

- Adrian, T.E., S.R. Bloom, K. Hermansen, and J. Iversen. 1978. Pancreatic polypeptide, glucagon and insulin secretion from the isolated perfused canine pancreas. *Diabetologia*. 14:413–417. <https://doi.org/10.1007/BF01228136>
- Alcolea, M.P., and P.H. Jones. 2014. Lineage analysis of epidermal stem cells. *Cold Spring Harb. Perspect. Med.* 4:a015206. <https://doi.org/10.1101/cshperspect.a015206>
- Al-Hasani, K., A. Pfeifer, M. Courtney, N. Ben-Othman, E. Gjernes, A. Vieira, N. Druelle, F. Avolio, P. Ravassard, G. Leuckx, et al. 2013. Adult duct-lining cells can reprogram into  $\beta$ -like cells able to counter repeated cycles of toxin-induced diabetes. *Dev. Cell*. 26:86–100. <https://doi.org/10.1016/j.devcel.2013.05.018>
- Alwan, A., 2010. Global Status Report on Noncommunicable Diseases. World Health Organization. 176 pp. Available at [http://www.who.int/nmh/publications/ncd\\_report2010/en/](http://www.who.int/nmh/publications/ncd_report2010/en/).
- Chera, S., D. Baronnier, L. Ghila, V. Cigliola, J.N. Jensen, G. Gu, K. Furuyama, F. Thorel, F.M. Gribble, F. Reimann, and P.L. Herrera. 2014. Diabetes recovery by age-dependent conversion of pancreatic  $\delta$ -cells into insulin producers. *Nature*. 514:503–507. <https://doi.org/10.1038/nature13633>
- Chiang, M.K., and D.A. Melton. 2003. Single-cell transcript analysis of pancreas development. *Dev. Cell*. 4:383–393. [https://doi.org/10.1016/S1534-5807\(03\)00035-2](https://doi.org/10.1016/S1534-5807(03)00035-2)
- Collombat, P., A. Mansouri, J. Hecksher-Sørensen, P. Serup, J. Krull, G. Gradwohl, and P. Gruss. 2003. Opposing actions of Arx and Pax4 in endocrine pancreas development. *Genes Dev.* 17:2591–2603. <https://doi.org/10.1101/gad.269003>
- Collombat, P., X. Xu, P. Ravassard, B. Sosa-Pineda, S. Dussaud, N. Billestrup, O.D. Madsen, P. Serup, H. Heimberg, and A. Mansouri. 2009. The ectopic expression of Pax4 in the mouse pancreas converts progenitor cells into  $\alpha$  and subsequently  $\beta$  cells. *Cell*. 138:449–462. <https://doi.org/10.1016/j.cell.2009.05.035>
- Courtney, M., E. Gjernes, N. Druelle, C. Ravaud, A. Vieira, N. Ben-Othman, A. Pfeifer, F. Avolio, G. Leuckx, S. Lacas-Gervais, et al. 2013. The inactivation of Arx in pancreatic  $\alpha$ -cells triggers their neogenesis and conversion into functional  $\beta$ -like cells. *PLoS Genet.* 9:e1003934. <https://doi.org/10.1371/journal.pgen.1003934>
- Edelstein, A.D., M.A. Tsuchida, N. Amodaj, H. Pinkard, R.D. Vale, and N. Stuurman. 2014. Advanced methods of microscope control using  $\mu$ Manager software. *J. Biol. Methods*. 1:10. <https://doi.org/10.14440/jbm.2014.36>
- Fink, J., A. Andersson-Rolf, and B.-K. Koo. 2015. Adult stem cell lineage tracing and deep tissue imaging. *BMB Rep.* 48:655–667. <https://doi.org/10.5483/BMBRep.2015.48.12.249>
- Gouzi, M., Y.H. Kim, K. Katsumoto, K. Johansson, and A. Grapin-Botton. 2011. Neurogenin3 initiates stepwise delamination of differentiating endocrine cells during pancreas development. *Dev. Dyn.* 240:589–604. <https://doi.org/10.1002/dvdy.22544>
- Hsu, Y.C. 2015. Theory and practice of lineage tracing. *Stem Cells*. 33:3197–3204. <https://doi.org/10.1002/stem.2123>
- Morrish, N.J., S.L. Wang, L.K. Stevens, J.H. Fuller, and H. Keen. 2001. Mortality and causes of death in the WHO Multinational Study of Vascular Disease in Diabetes. *Diabetologia*. 44(S2, Suppl 2):S14–S21. <https://doi.org/10.1007/PL00002934>
- Pan, F.C., E.D. Bankaitis, D. Boyer, X. Xu, M. Van de Castele, M.A. Magnuson, H. Heimberg, and C.V.E. Wright. 2013. Spatiotemporal patterns of multipotentiality in Ptf1a-expressing cells during pancreas organogenesis and injury-induced facultative restoration. *Development*. 140:751–764. <https://doi.org/10.1242/dev.090159>
- Pascolini, D., and S.P. Mariotti. 2012. Global estimates of visual impairment: 2010. *Br. J. Ophthalmol.* 96:614–618. <https://doi.org/10.1136/bjophthalmol-2011-300539>
- Prado, C.L., A.E. Pugh-Bernard, L. Elghazi, B. Sosa-Pineda, and L. Sussel. 2004. Ghrelin cells replace insulin-producing beta cells in two mouse models of pancreas development. *Proc. Natl. Acad. Sci. USA*. 101:2924–2929. <https://doi.org/10.1073/pnas.0308604100>
- Roncoroni, L., V. Violi, M. Montanari, and M. Muri. 1983. Effect of somatostatin on exocrine pancreas evaluated on a total external pancreatic fistula of neoplastic origin. *Am. J. Gastroenterol.* 78:425–428.
- Schindelin, J., I. Arganda-Carreras, E. Frise, V. Kaynig, M. Longair, T. Pietzsch, S. Preibisch, C. Rueden, S. Saalfeld, B. Schmid, et al. 2012. Fiji: an open-source platform for biological-image analysis. *Nat. Methods*. 9:676–682. <https://doi.org/10.1038/nmeth.2019>
- Soriano, P. 1999. Generalized lacZ expression with the ROSA26 Cre reporter strain. *Nat. Genet.* 21:70–71. <https://doi.org/10.1038/5007>
- Sosa-Pineda, B., K. Chowdhury, M. Torres, G. Oliver, and P. Gruss. 1997. The Pax4 gene is essential for differentiation of insulin-producing beta cells in the mammalian pancreas. *Nature*. 386:399–402. <https://doi.org/10.1038/386399a0>
- Taniguchi, H., M. He, P. Wu, S. Kim, R. Paik, K. Sugino, D. Kvitsiani, Y. Fu, J. Lu, Y. Lin, et al. 2011. A resource of Cre driver lines for genetic targeting of GABAergic neurons in cerebral cortex. *Neuron*. 71:995–1013. <https://doi.org/10.1016/j.neuron.2011.07.026>
- World Health Organization. 2016. Global Report on Diabetes. Available at: <http://www.who.int/diabetes/global-report/en/> (accessed October 2, 2017).
- Xu, X., J. D’Hoker, G. Stangé, S. Bonné, N. De Leu, X. Xiao, M. Van de Castele, G. Mellitzer, Z. Ling, D. Pipeleers, et al. 2008.  $\beta$  cells can be generated from endogenous progenitors in injured adult mouse pancreas. *Cell*. 132:197–207. <https://doi.org/10.1016/j.cell.2007.12.015>
- Zhang, J., L.B. McKenna, C.W. Bogue, and K.H. Kaestner. 2014. The diabetes gene Hhex maintains  $\delta$ -cell differentiation and islet function. *Genes Dev.* 28:829–834. <https://doi.org/10.1101/gad.235499.113>